OPEN ACCESS
JOURNAL OF ADVANCED DIELECTRICS
Vol. 13, No. 4 (2023) 2341003 (7 pages)

DOI: 10.1142/S2010135X23410035

Orientation dependence on piezoresponse of lead-free piezoelectric sodium bismuth titanate epitaxial thin films

Jinyan Zhao*,‡,¶, Wei Ren*,§,¶, Zhe Wang*, Gang Niu*,
Lingyan Wang* and Yulong Zhao†

*Electronic Materials Research Laboratory, Key Laboratory of the Ministry of Education & International Center for Dielectric Research
School of Electronic Science and Engineering, Xi'an, P. R. China

†State Key Laboratory for Mechanical Manufacturing System
Xi'an Jiaotong University, Xi'an 710049, P. R. China

‡zhaojy7@xjtu.edu.cn
§wren@mail.xjtu.edu.cn

Received 12 September 2022; Revised 30 December 2022; Accepted 7 February 2023; Published 27 June 2023

Lead-free piezoelectric sodium bismuth titanate ($(Bi_{0.5}Na_{0.5})TiO_3$, BNT) thin films were epitaxially grown onto (001)-, (110)-, and (111)-oriented Nb:$SrTiO_3$ (STO) single crystal substrates prepared by sol–gel processing. Highly oriented growth in (001), (110), and (111) BNT thin films was obtained in this work benefiting from the lattice match between the BNT film and the STO substrate. The different growth models in thin films with various orientations result in various surface morphologies dependent on the film orientation. The piezoresponse of the BNT thin films was represented exhibiting a strong orientation dependence that (110)>(001)>(111). This is contributed by the various domain switching contribution related to the crystal symmetry and polarization distribution in the three oriented thin films.

Keywords: Sodium bismuth titanate; lead-free; orientation dependence; thin films; piezoelectric properties.

1. Introduction

Piezoelectric materials have been widely researched due to their extensive application in transducers, actuators, sensors, and memories. However, it is well known that the materials used for the applications above are still mainly dependent on lead-based piezoelectrics. However, lead-based compounds are currently being restricted in the industry because of the toxicity of lead in the preparation and use process. Therefore, it is essential to develop lead-free piezoelectric materials with high performance as alternatives for lead-based compounds. On this occasion, sodium bismuth titanate ($(Bi_{0.5}Na_{0.5})TiO_3$, BNT), lead-free piezoelectric materials with perovskite structure, has been recognized as a promising choice for application in the actuators.[1,2]

BNT thin film with excellent performance is in demand with device miniaturization and integration development. More significant piezoelectric properties obtained in single crystals than in ceramics benefit by eliminating grain boundaries and cutting in particular directions.[3] The limited electrical properties in the polycrystalline thin films prevent the BNT film from being applied to the devices.[4–6] Epitaxial thin films may have higher piezoelectric properties than polycrystalline thin films due to anisotropic properties in piezoelectrics. Research on epitaxial BNT thin films makes it more hopeful for device applications. It was reported that the preferred orientation texture of (111)-oriented BNT films deposited on (111) Pt/Ti/SiO_2/Si substrates prepared by the sol–gel technique is 71.5%.[7] The preferred orientation of (111) BNT thin film grown on Pt substrate by Pulsed Laser Deposition (PLD) method exhibits some grains in (001) and (110) directions.[8] BNT films with (100) preferred orientation deposited on (100)MgO substrates using the PLD method have a weak (110) peak existing in XRD 2θ results.[9] The (110) preferentially oriented BNT film deposited on the (110) Pt/(110)$SrTiO_3$ substrate by the PLD method has weak (100) and (111) peaks.[10] There is still a limitation in the fabrication of high-quality epitaxial BNT thin films.

The piezoelectric performance largely relies on the crystallization direction and poling direction of materials. The piezoelectric coefficient in the BNT-based single crystals with rhombohedral phase exhibits a relation to the orientation that (110) > (001) > (111).[11] The piezoelectricity of single crystal films also closely depends on the film orientation. The $0.775(Bi_{0.5}Na_{0.5})TiO_3$–$0.065BaTiO_3$–$0.18SrTiO_3$ (BNT–BT–ST) single crystal thin films fabricated on

¶Corresponding authors.

$Nb:SrTiO_3$ substrate by a sol–gel technique exhibited a relationship between the piezoelectric and orientations that (001) < (110) < (111).[12] The piezoelectric coefficients in the $K_{0.5}Na_{0.5}NbO_3$ (KNN) single crystal thin films with different orientations fabricated by the sol–gel technique on Nb-doped STO substrates with various orientations are (001) > (110) > (111).[13] Therefore, there is a need to urgently study the relationship between the piezoelectric properties and orientation direction in thin films.

In this work, (001)-, (110)-, and (111)-oriented BNT epitaxial films were prepared on $Nb:SrTiO_3$ (Nb:STO) substrates by a chemical solution deposition method. The crystallographic nature and the piezoresponse of the BNT epitaxial thin films were investigated.

2. Experimental Procedure

The BNT thin films were prepared using the chemical solution deposition method. The raw materials including tetrabutyl titanate (97%, Sigma-Aldrich), bismuth nitrate (99%, Alfa-Aesar), and sodium acetate (99%, Sigma-Aldrich) were used in this work. Stoichiometric starting materials were dissolved in the 2-methoxyethanol (analytical pure, Sinopharm Chemical Reagent), and a small quality of acetic acid (99.5%, Sinopharm Chemical Reagent) was added as a solvent. Acetylacetone (99%, Sinopharm Chemical Reagent) was added as a polymerizing agent to avoid the hydrolyzation of tetrabutyl titanate. There is an excess of 2 mol.% Bi and 10 mol.% Na in the precursor solution to compensate for the evaporation of bismuth and sodium compounds during film deposition. The solution was stirred at 80°C for 1 h, and the final solution concentration was 0.3 mol/L. The BNT solution was spin-coated on (001)-, (110)-, and (111)-oriented Nb:STO substrates at 3000 revolutions per second, and the films were obtained after being thermally treated in a rapid thermal annealing furnace at 150°C for 3 min, at 420°C for 10 min, and annealed at 750°C for 5 min. Detailed information was introduced in our previous work.[14] The spin-coating deposition process and heat treatment were repeated until the designed thickness was obtained. The structural and electrical properties of BNT thin films with a thickness ranging from 250 nm to 260 nm (six deposited layers, 6L) deposited on (001)-, (110)-, and (111)-oriented Nb:STO substrates are presented in this work. The structural properties of thin films with 1L and 3L deposited on the (001)-oriented Nb:STO substrates are also shown.

A diffractometer (Xpert pro MRD Modern Globe) with Cu Kα1 radiation (λ = 1.5406 Å) was used to characterize the crystalline phase of the thin films including out-of-plane θ–2θ scans, in-plane φ scans, and Reciprocal Space Mapping (RSM). Field-emission scanning electron microscopy (FESEM, Quanta 250 FEG, FEI, Japan) was used to characterize the surface and cross-sectional morphologies. The elemental distributions of the thin films and substrate were analyzed through transmission electron microscopy (TEM, JEOL JEM 2100F, Japan) and energy dispersive spectroscopy (EDS). For TEM and EDS measurements, a thin slice of 5*5 μm was cut via a focused ion beam (FIB, Zeiss Crossbeam 540, Germany). The domain structure and the piezoresponse were carried out by piezoresponse force microscopy (PFM, Dimension Icon, Bruker, USA). The bottom electrode of the thin film was attached to the sample stage using silver paste. A conductive tip (Bruker, SCM-PIT) mounted on a cantilever was regarded as the top electrode. An ac bias (f: 54 kHz, A: 4 V) was applied to the bottom electrode to drive the thin film. A triangular wave with an amplitude of 20 V was applied to the conductive tip to characterize the phase and amplitude hysteresis loops by being equipped with a voltage amplifier.

3. Results and Discussion

The X-ray diffraction θ–2θ patterns of (001)-oriented BNT thin films with different deposited layers are presented in Fig. 1(a). It can be seen that the (001) and (002) peaks of the films are located at higher angles than the substrates. The films with different thicknesses grow in strict accordance with the orientation of the substrates. The intensity of the (001)-oriented BNT thin films increases with increasing thickness. Since a good orientation was obtained in the 6L films, the following present the results of thin films with six layers deposited on different oriented substrates.

Figure 1(b) shows the X-ray diffraction θ–2θ patterns of (001)-, (110)-, and (111)-oriented BNT thin films deposited on the corresponding oriented Nb:STO substrates. A perovskite structure with single-phase and enhanced peak intensity following the orientations of single-crystalline substrates is observed in all the samples. The formation of such highly oriented growth in all three oriented films profits from the fact that the film compounds and the substrate have close lattice parameters. The lattice parameters of the BNT powder with rhombohedral phase and the Nb:STO substrate are 0.3886 nm and 0.3905 nm, respectively. Moreover, the thermal expansion coefficient of BNT material is 11 ppm/K, comparable to that of STO (11.7 ppm/K). When the film is prepared from high temperature to low temperature, the film is subject to very little thermal stress. The (001)-, (110)-, and (111)-oriented BNT thin films deposited on Nb:STO substrates exhibit outstanding crystalline characteristics and highly oriented growth compared to the previous works.[7,8] The (001) and (002) diffraction peaks of the (001)-oriented BNT thin films locate at a higher degree than the corresponding peaks of the Nb:STO substrate, indicating that the film has smaller unit cell than that of the substrate, the same goes for the (011)- and (111)-oriented films.

The in-plane texturing of the (001) and (111) BNT thin films was confirmed by the XRD φ-scan. Figure 1(c) presents the (001) BNT thin films on the substrate. The lower part is the φ scan result of the BNT thin film, and the upper part is the φ scan result of the (001) Nb:STO substrate. The in-plane

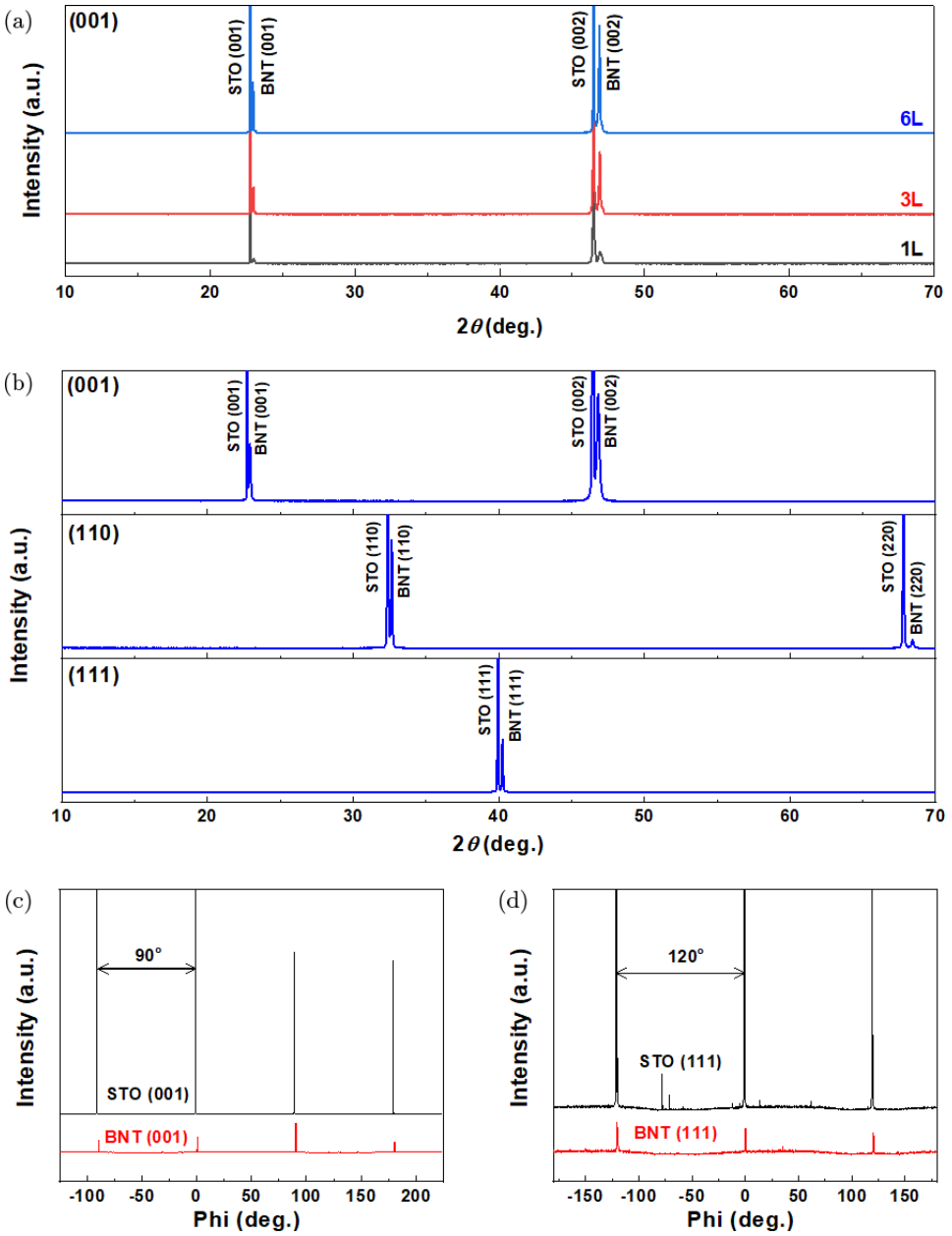

Fig. 1. (a) The X-ray diffraction θ–2θ patterns of (001)-oriented BNT thin films with thicknesses of 1L, 3L, and 6L; (b) the X-ray diffraction θ–2θ patterns of (001)-, (110)-, and (111)-oriented BNT thin films with 6L; (c) the in-plane φ scanning results of (001) and (d) (111) films with 6L.

symmetry of the film is the same as that of the substrate, which is quadruple symmetry wherein four symmetries with uniformly separated peaks can be found. Figure 1(d) shows the in-plane φ scanning results of (111) BNT thin film. The upper part of the figure refers to the φ scan results of the STO substrate, and the lower part is the φ scan results of the BNT film. The in-plane symmetry of the film is the same as that of the substrate with triple symmetry, indicating an epitaxial growth of the film strictly according to the substrate lattice. The results confirm a nonlattice-rotated epitaxial relationship between the BNT thin films and the STO substrates in both (001)- and (111)-oriented thin films. The φ scanning result of (110) BNT film is not shown here. It isn't easy to distinguish the diffraction peak of the film from that of the substrate due to the lattice match between them.

The RSM was measured on the (103) scattering surface of the (001)-oriented film and substrate, and the results are shown in Fig. 2. The film exhibits comparable in-plane lattice parameters to that of the substrate. While the out-of-plane lattice parameter of the film is different from that of the substrate along the direction [001]. The schematic diagram of the unit cell and the stress condition of the (001)-oriented

Table 1. The lattice parameters of the (001)-oriented BNT thin film, Nb:STO substrate, and BNT powder.

	BNT film		STO substrate	BNT powder	Lattice mismatch/%
	a/nm	*c*/nm	*a*/nm	*a*/nm	
Lattice parameters	0.3894	0.3871	0.3905	0.3886	0.28

BNT film is shown in Figs. 2(b) and 2(c). Define c as the out-of-plane lattice parameter along [001] and a as the in-plane lattice parameter along [100]. The lattice parameters of (001)-oriented BNT thin film are determined from the RSM results (c is 0.3871 nm and a is 0.3894 nm), as shown in Table 1. The lattice parameters of BNT gel powder and STO are 0.3886 nm and 0.3905 nm, respectively. The a-axis length is stretched, and the c-axis size is compressed due to the tensile stress from the substrate.

The lattice mismatch can be calculated by the formula:

$$\delta(\%) = \frac{d_f - d_{\text{sub}}}{d_{\text{sub}}} \times 100,$$

where δ is the Lattice mismatch coefficient, d_f is the Lattice constant of thin films, and d_{sub} is the Lattice constant of the substrate.

According to the equation above, the lattice mismatch coefficient of thin film and substrate along (001) surface is 0.28%.

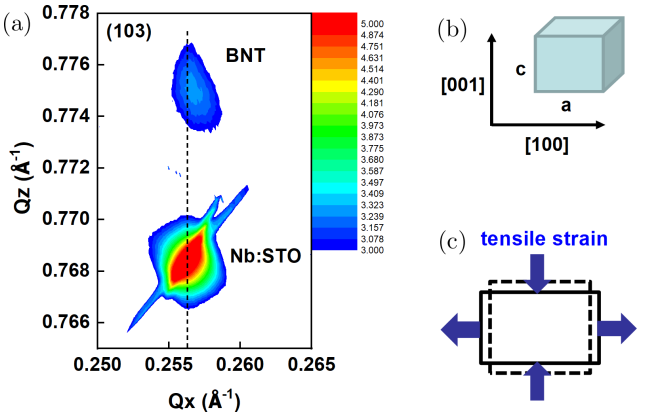

Fig. 2. The RSM on the (103) scattering surface, (b) the schematic diagram of the unit cell, and (c) the stress condition of the (001)-oriented BNT thin film.

To investigate the elemental distribution in the film and the interface, the (001) thin film was analyzed via a mapping and a line profile using EDS. Figure 3(a) shows the cross-sectional TEM image and the corresponding Na, Bi, and Sr element mapping images. A sharp interface can be observed in the TEM and EDS mapping images. Na and Bi elements are detected in the film, and the Sr element is detected in the substrate. No elements diffusion was observed. Figure 3(b) displays the line profile of Na, Bi, and Sr elements along the

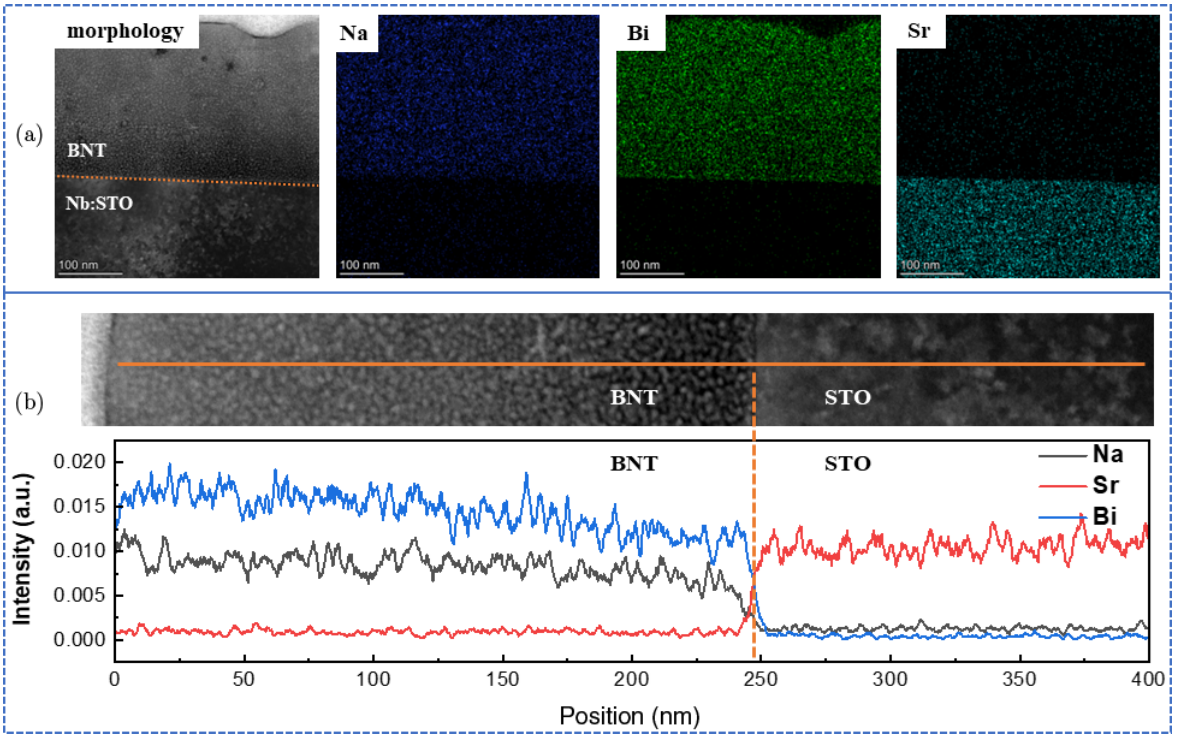

Fig. 3. (a) Cross-sectional TEM image of the (001)-oriented BNT thin film and EDS mapping profile of an elemental distribution along the cross-sectional image. (b) EDS line profile of an elemental distribution along the depth of the (001) BNT film, including the line profile across the film and substrate by EDS.

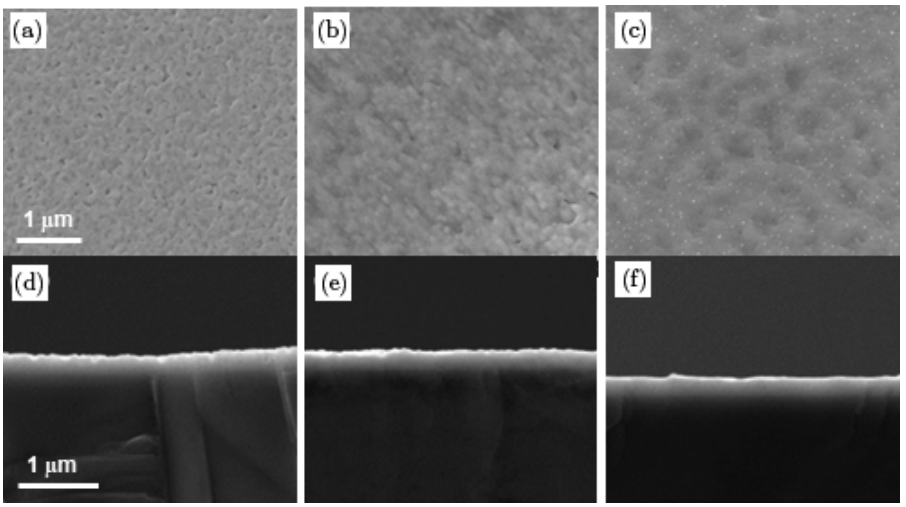

Fig. 4. The surface SEM images of the (a) (001)-, (b) (110)-, and (c) (111)-oriented BNT films; the cross-sectional SEM images of the (d) (001)-, (e) (110)- and (f) (111)-oriented BNT films.

depth of the cross-sectional image. The line profile was measured along the orange line in the scanning image. The elemental distribution was consistent in the film and substrate with a sharp change in the interface.

Figure 4 shows the surface and cross-sectional SEM morphologies of (001), (110), and (111) BNT thin films. All the films grow closely and orderly along the substrate STO with a dense structure. The thicknesses of (001)-, (110)-, and (111)-oriented BNT thin films were calculated to be 250, 260, and 250 nm according to the cross-sectional images, respectively. The different oriented films exhibit various surface morphologies. The (001)-oriented film reveals a granular and tightly arranged, the (001)-oriented film shows strip-like grains, and the (111)-oriented film surface is distributed as island-like clusters. Combined with the surface morphologies of the thin films and Winterbottom configuration theory,[15] it can be found that the (001)-oriented BNT film follows a layer-by-layer growth, the (110)-oriented BNT film grows in strips, and the (111)-oriented BNT film shows island growth.

The polarization distribution and piezoelectric properties in local scale were investigated by PFM. As shown in Figs. 5(a)–5(c), the (001)-, (110)-, and (111)-oriented BNT thin films exhibit homogenous phase images with a single polarization direction, indicating a self-polarization in the films, which was reported in some polycrystalline and monocrystalline BNT thin films induced by the built-in electric field.[14,16,17] Figures 5(d)–5(f) present the phase switching curves of the (001)-, (110)-, and (111)-oriented BNT thin films. When the applied electric field changes from a negative voltage to a positive voltage, the phase turns 180°, indicating that the polarization direction of the film is switchable by using an external electric field. Well-shaped piezoresponse amplitude butterfly loops are obtained for (100)-, (110)-, and (111)-oriented BNT thin films, as shown in Figs. 5(h) –5(j). Although there is no exact calibration for the piezoresponse measurements, the measurement condition for the three films was exactly the same. The measurements were carried out using one conductive tip, the same laser position, and the same operating parameters, including setpoint, driving frequency, and drive amplitude. It is no problem to compare the relative displacement of the films. The piezoresponse exhibits anisotropic according to the orientation that (110)>(001)>(111). The piezoelectric response in the (100)- and (110)-oriented BNT thin films is vastly higher than that in the (111)-oriented BNT thin films.

Next, the reasons for the anisotropic piezoelectric response in films with different orientations are discussed. It is believed that the piezoelectric properties in piezoelectric films are highly dependent on the characteristics of the domain structures and domain walls.[15] Two factors contribute to the piezoelectric response in ferroelectric thin films: the intrinsic factor related to the lattice deformation and the extrinsic non-180° domain reversal associated with the elastic deformation coming from domain wall motion. The extrinsic contribution is the main factor affecting the piezoelectric response of thin films because the lattice deformation has a minor effect in thin films with limited thickness.[13]

The schematic diagram of the polarization switching behavior in the (a) (001)-, (b) (110)-, and (c) (111)-oriented BNT thin films is shown in Fig. 6. The BNT material is a rhombohedral phase (R3c) structure,[18] and the spontaneous polarization is along the body diagonal direction of the cell. There are eight possible directions of spontaneous polarization in a single cell. Three kinds of domains with 71°, 109°, and 180° exist in the system. The rhombohedral unit cell was treated as a pseudocubic one for simplicity in Fig. 6. The solid red arrow means the spontaneous polarization direction, the dark dotted arrow means no spontaneous polarization along the direction, and the dark solid arrow refers to the switched polarization direction. As mentioned in Fig. 5, all films exhibit self-polarization with polarization toward the bottom. The spontaneous polarization

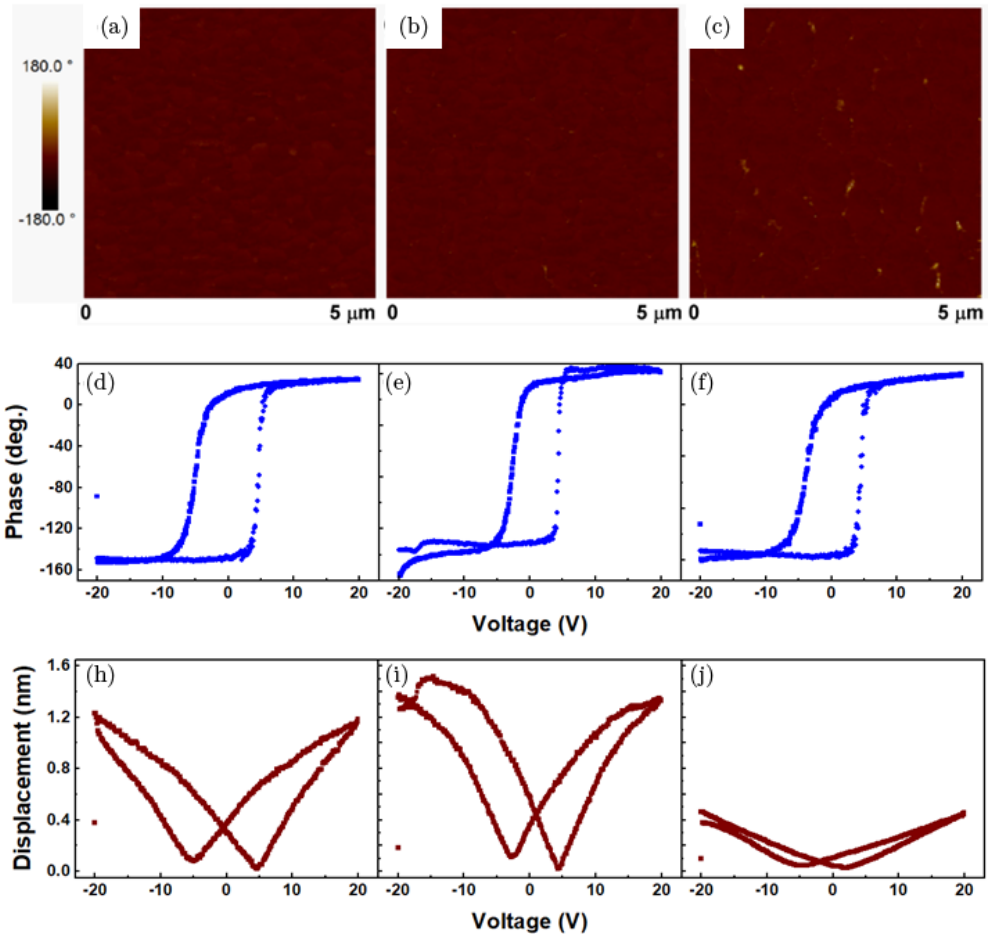

Fig. 5. The piezoresponse phase images of the (a) (001)-, (b) (110)-, and (c) (111)-oriented BNT thin films, the phase switching curves of the (d) (001)-, (e) (110)-, and (f) (111)-oriented BNT films, and the displacement butterfly-like hysteresis loops of the (h) (001)-, (i) (110)-, and (j) (111)-oriented BNT films measured by PFM.

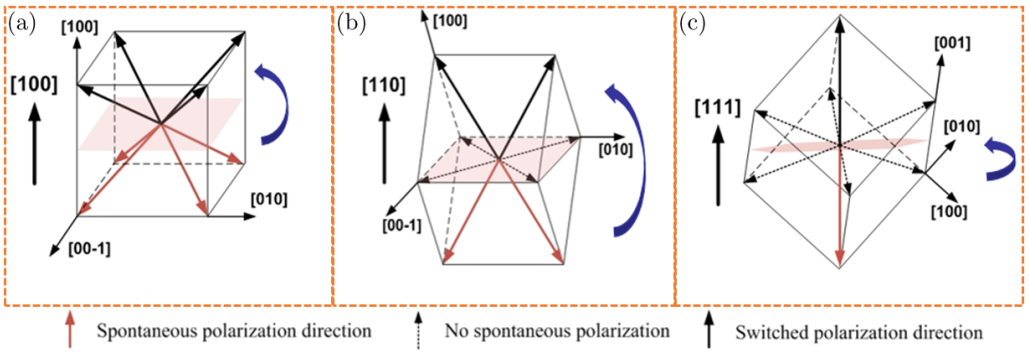

Fig. 6. The schematic diagram of the polarization switching behavior in the (a) (001)-, (b) (110)-, and (c) (111)-oriented BNT thin films.

is possible along the four diagonal bottom directions marked as solid red arrows in the (001)-oriented thin film, as shown in Fig. 6(a). When an upward electric field is applied, the polarization is turned to the four inclined top directions marked as solid dark arrows. 180° and 71° domain switching occurs in the (001)-oriented thin film. The spontaneous polarization is possible along the two diagonal bottom directions marked as solid red arrow in the (110)-oriented thin film as shown in Fig. 6(b). When an upward electric field is applied, the polarization is turned to the two inclined top directions marked as solid dark arrows. 180° and 109° domain switching occurs in the (110)-oriented thin film. The spontaneous polarization is only possible along the one direction toward the bottom marked as a solid red arrow in the (111)-oriented thin film, as shown in

Fig. 6(c). When an upward electric field is applied, the polarization is turned upward along the electric field marked as a solid dark arrow. Only 180° domain switching happens in the (111)-oriented thin film. Non-180° domain reversal causes the domain wall motion, and there is no domain wall motion in the 180° domain switching process. When the electric field is applied, the domain wall motion contributes the largest in the (110) film to the piezoelectric response, followed by the (100) film, and without the contribution of the domain wall motion in the (111) film. Therefore, the (111)-oriented thin film exhibits a much smaller piezoresponse than that in the (001)- and (110)-oriented thin films. The piezoelectric response of BNT film depends on the orientation of the film, and the size relationship is (110)>(100)>(111). The films grown along the nonpolar axes exhibit a much larger piezoelectric constant than that in the film grown along the polar directions.[12,13,15] It was reported that the piezoelectric coefficient along <110> and <001> directions is the highest in BNT single crystals.[11] The result of the oriented film is consistent with the characteristics of a single crystal.

4. Conclusion

In conclusion, the epitaxial BNT thin films have been successfully deposited on Nb:STO single-crystalline substrates with (001), (110), and (111) orientations by the chemical solution deposition method. The films grown along the nonpolar axes exhibit a much larger piezoelectric constant than that in the film grown along the polar directions benefiting from the domain engineering. The (110)-oriented BNT thin film exhibits the highest piezoresponse, making the epitaxial BNT thin film a promising candidate for actuator applications.

Acknowledgments

This work was supported by the Natural Science Foundation of China (Grant No. 51902246), the Natural Science Fundamental Research Project of Shaanxi Province of China (No. 2019JQ590), the Fundamental Research Funds for the Central Universities, and the "111 Project" of China (B14040). We acknowledge Mrs. Yanzhu Dai and Mr. Hu Nan at the Electronic Materials Research Laboratory, Key Laboratory of the Ministry of Education & International Center for Dielectric Research of Xi'an Jiaotong University, for the assistance with SEM measurement. We acknowledge the support of Xijiang Innovation Team Introduction Program of Zhaoqing (Jiecheng).

References

[1]J. Rödel and J. F. Li, Lead-free piezoceramics: Status and perspectives, *MRS Bull.* **43**(8), 576 (2018).
[2]J. Rödel, W. Jo, K. T. Seifert, E. M. Anton, T. Granzow and D. Damjanovic, Perspective on the development of lead-free piezoceramics, *J. Am. Ceram. Soc.* **92**(6), 1153 (2009).
[3]H. Fu and R. E. Cohen, Polarization rotation mechanism for ultrahigh electromechanical response in single-crystal piezoelectrics, *Nature* **403**(6767), 281 (2000).
[4]W. Sakamoto, N. Makino, B. Y. Lee, T. Iijima, M. Moriya and T. Yogo, Influence of volatile element composition and Mn doping on the electrical properties of lead-free piezoelectric $(Bi_{0.5}Na_{0.5})TiO_3$ thin films, *Sens. Actuators A: Phys.* **200**, 60 (2013).
[5]M. Suzuki, Y. Noguchi, M. Miyayama and J. Akedo, Polarization and leakage current properties of bismuth sodium titanate ceramic films deposited by aerosol deposition method, *J. Ceram. Soc. Jpn.* **118**(1382), 899 (2010).
[6]T. Yu, K. W. Kwok and H. L. W. Chan, Preparation and properties of sol–gel-derived $Bi_{0.5}Na_{0.5}TiO_3$ lead-free ferroelectric thin film, *Thin Solid Films* **515**(7–8), 3563 (2007).
[7]X. G. Tang, J. Wang, X. X. Wang and H. L. W. Chan, Preparation and electrical properties of highly (111)-oriented $(Na_{0.5}Bi_{0.5})TiO_3$ thin films by a sol–gel process, *Chem. Mater.* **16**(25), 5293 (2004).
[8]J. R. Duclere, C. Cibert, A. Boulle, V. Dorcet, P. Marchet, C. Champeaux, A. Catherinot, S. Deputier and M. Guilloux-Viry, Lead-free $Na_{0.5}Bi_{0.5}TiO_3$ ferroelectric thin films grown by Pulsed Laser Deposition on epitaxial platinum bottom electrodes, *Thin Solid Films* **517**(2), 592 (2008).
[9]M. Bousquet, J. R. Duclere, C. Champeaux, A. Boulle, P. Marchet, A. Catherinot, A. Wu, P. M. Vilarinho, S. Deputier, M. Guilloux-Viry, A. Crunteanu, B. Gautier, D. Albertini and C. Bachelet, Macroscopic and nanoscale electrical properties of pulsed laser deposited (100) epitaxial lead-free $Na_{0.5}Bi_{0.5}TiO_3$ thin films, *J. Appl. Phys.* **107**(3), 104107 (2010).
[10]M. Bousquet, J. R. Duclere, B. Gautier, A. Boulle, A. Wu, S. Deputier, D. Fasquelle, F. Remondiere, D. Albertini, C. Champeaux, P. Marchet, M. Guilloux-Viry and P. Vilarinho, Electrical properties of (110) epitaxial lead-free ferroelectric $Na_{0.5}Bi_{0.5}TiO_3$ thin films grown by pulsed laser deposition: Macroscopic and nanoscale data, *J. Appl. Phys.* **111**(10), 104106 (2012).
[11]D. Schneider, W. Jo, J. Rödel, D. Rytz and T. Granzow, Anisotropy of ferroelectric behavior of $(1-x)Bi_{1/2}Na_{1/2}TiO_3$–$xBaTiO_3$ single crystals across the morphotropic phase boundary, *J. Appl. Phys.* **116**(4), 044111 (2014).
[12]W. Li, P. Li, H. R. Zeng, J. G. Hao and J. W. Zhai, Orientation dependence on piezoelectric properties of $Bi_{0.5}Na_{0.5}TiO_3$–$BaTiO_3$–$SrTiO_3$ epitaxial thin films, *Appl. Phys. Lett.* **104**(17), 172903 (2014).
[13]Q. Yu, J. F. Li, W. Sun, Z. Zhou, Y. Xu, Z. K. Xie, F. P. Lai and Q. M. Wang, Electrical properties of $K_{0.5}Na_{0.5}NbO_3$ thin films grown on Nb:$SrTiO_3$ single-crystalline substrates with different crystallographic orientations, *J. Appl. Phys.* **113**(2), 024101 (2013).
[14]J. Zhao, G. Niu, W. Ren, L. Wang, G. Dong, N. Zhang, M. Liu and Z. G. Ye, Self-polarization in epitaxial fully matched lead-free bismuth sodium titanate based ferroelectric thin films, *ACS Appl. Mater. Interfaces* **10**(28), 2 (2018).
[15]B. C. Luo, D. Y. Wang, M. M. Duan and S. Li, Orientation-dependent piezoelectric properties in lead-free epitaxial $0.5BaZr_{0.2}Ti_{0.8}O_3$–$0.5Ba_{0.7}Ca_{0.3}TiO_3$ thin films, *Appl. Phys. Lett.* **103**(12), 122903 (2013).
[16]J. Y. Zhao, W. Ren, G. Niu, N. Zhang, G. H. Dong, L. Y. Wang, M. Liu, P. Shi and Z. G. Ye, Recoverable self-polarization in lead-free bismuth sodium titanate piezoelectric thin films, *ACS Appl. Mater. Interfaces* **9**(34), 28716 (2017).
[17]J. Zhao, G. Niu, W. Ren, L. Wang and Y. Zhao, Polarization behavior of lead-free $0.94(Bi_{0.5}Na_{0.5})TiO_3$–$0.06BaTiO_3$ thin films with enhanced ferroelectric properties, *J. Eur. Ceram. Soc.* **40**(12), 3928 (2020).
[18]G. A. Smolenskii, V. A. Isupov, A. I. Agranovskaya and N. N. Krainik, New ferroelectric of complex composition, *Sov. Phys. — Solid State* **2**(11), 2651 (1961).